Reviews & Papers

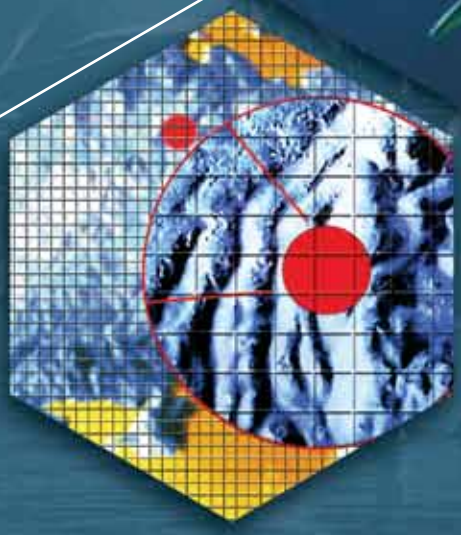

From the Technical Editor

Humans are hungry for energy. More use from traditional sources is coming at a cost to the environment but we are starting to look for alternatives. Our ideal sources will convert the energy created within the environment to something that will be useful to us, or even better, saleable. This approach should have advantages over consumable forms of energy, in that we will not exhaust the supply of raw material.

Wind, waves, tidal, solar and geothermal energy sources are available from the oceans but each of these sources requires a special technology to convert it to a saleable commodity. The amount of available natural energy depends very specifically on the physical site, and wind, waves and solar energy are not available at constant rates. Supplies of geothermal and tidal energy are more predictable but they are restricted to very specific locations where the energy concentrations are high enough to be commercially viable.

For alternative energy sources to be successful, we need the combination of three things. First there is society's need to change its source of energy supply due to capacity limits, environmental concerns or national security reasons. Second, we need technologies that can reliably convert the natural energy into the saleable kind. This includes the ability of the physical plant to withstand the environmental forces in exposed locations, grids of wires to take the energy from its source to the market, and the ability to blend energy from different sources. Finally, we need the whole system to be economically viable, so that the cost of production is competitive with the 'dirty' alternatives.

We must be responsible in how we apply our renewable technology ideas as well. The very act of building something to harvest the energy will change the environment around it. For example, sediment patterns around beaches may change if wave energy devices are built. Wind turbines may have an effect on birds and fish may be affected by turbines in rivers and tidal flows. Also, not everyone will accept that renewable energy is desirable in their back yard. For example, there has sometimes been a reluctance to support wind turbines being built onshore, where they interfere with the natural beauty of the proposed location. This has led to the demand for offshore wind turbines with more complex technical challenges.

To make renewable energy accepted, we need policies from all levels of government to encourage the use of renewable energy. This should include more research into technology and also research into the economics of production and minimizing the impact of these installations on the world around us. Renewable energy should come at the least cost to the whole planet, and not the least cost to the rich regions, with no benefit to the disadvantaged.

Dr. David Molyneux
Technical Editor

Thank you to our Reviewers!

Each and every technical paper submitted to *The Journal of Ocean Technology* undergoes an extensive peer review by our volunteer reviewers – ocean technology experts located around the globe. Their input is extremely valuable in helping make decisions on publication and maintaining the high standards expected from our authors. As an expression of our appreciation and gratitude for their efforts and input, we want to publicly thank each and every volunteer reviewer.

Mehmet Atlar
University of Newcastle-Upon-Tyne
Emile Baddour
National Research Council
Don Bass
Memorial University of Newfoundland
Eric Bibeau
University of Manitoba
Matt Broadhurst
National Marine Science Centre
Sofia Caires
Delft Hydraulics
Sander Calisal
University of British Columbia
Bruce Colbourne
National Research Council of Canada
Scott Couch
Edinburgh University
John Cross
Fisheries and Marine Institute
Claude Daley
Memorial University of Newfoundland
Ahmed Derradji
National Research Council
Lawrence Doctors
University of New South Wales
Timothy Duda
Woods Hole Oceanographic Institution
Thierry Faure
National Research Council
James Ferguson
International Submarine Engineering Ltd.
Hassan Ghassemi
Amirkabir University of Technology
Ada Gotman
Novosibirsk State Academy of
Water Transport
Gwyn Griffiths
University of Southampton
Mahmoud Haddara
Memorial University of Newfoundland
Moquin He
National Research Council
Mike Hinchey
Memorial University of Newfoundland
Alan Hughes
Southampton National Oceanography Centre
Tariq Iqbal
Memorial University of Newfoundland
Daniel Jones
University of Southampton
Emma Jones
National Institute of Water and
Atmospheric Research Limited
Andrew Kendrick
Fleetech.com
Myung Hyun Kim
Pusan National University
Cesar Levy
Florida International University
Cho-Chung Liang
Da-Yeh University
Pengfei Liu
National Research Council
Gregor Macfarlane
Australian Maritime College
John MacKay
Defence Research and Development Canada
James Miller
University of Rhode Island
Sue Molloy
Glas Ocean Engineering
Dave Murrin
Memorial University of Newfoundland
Ioan Nistor
University of Ottawa
F. (Barry) O'Neill
Fisheries Research Services
Neil Pegg
Defence Research and Development Canada
Irene Penesis
Australian Maritime College
Fernando Ponta
Michigan Technological University
Shin Rhee
Seoul National University
Kiyoshi Shimada
Akishima Laboratories (Mitsui Zosen) Inc.
Kostas Spyrou
National Technical University of Athens
Dave Stredulinksy
Defence Research and Development Canada
Christina Wang
ABS Houston
Xiaolan Wang
Environment Canada
George Watt
Defence Research Development Canada
Goran Wilkman
akeryards.com
Stefan Williams
University of Sydney
Paul Winger
Fisheries and Marine Institute
Fraser Winsor
National Research Council
Ali Yousefpour
National Research Council

Thank You

A wavy retrospective

Grégory S. Payne

Jamie R.M. Taylor

David Ingram

Payne, Taylor and Ingram give a comprehensive overview of methodologies for the tank testing of wave energy converter (WEC) models, including a summary of best practice guidelines for three elements: the physical model, measurements and wave generation.

Who should read this paper?

Anyone whose work involves the development and marketing of wave energy conversion devices, or the physical reproduction of ocean wave conditions at reduced scale, or understanding the variability and structure of ocean waves should find this paper of interest. In addition, those involved in the creation or purchase of new test tank facilities will find it useful.

Why is it important?

Tank testing is commonly used to investigate the impact of different configurations, dimensions and other key design parameters of wave energy converters influencing their predicted performance, cost and environmental impact. The WEC models that are put into such tanks must be able to accurately simulate at milliwatt-scale the dynamic behaviour of potential full-scale megawatt devices. This paper distills experience gained and methodologies developed at the leading wave energy model testing centres since the mid 1970s. Many of the instruments and techniques used in wave energy tank testing have been developed in relative isolation from traditional ocean engineering and naval architecture disciplines. It is intended that the discussion presented here will help to spread knowledge from this specialist area into the greater communities of test tank users and ocean engineers. At the same time it may also encourage the flow of useful insights from this wide community back to wave energy specialists.

About the authors

Dr. Grégory Payne is a research associate in the Institute for Energy Systems, School of Engineering, University of Edinburgh. His research interests include wave tank testing, instrumentation and numerical modeling of wave energy converters.

Jamie Taylor is a Senior Research Fellow at the University of Edinburgh with interests across the renewable energy spectrum. From the mid 1970s, he worked with Professor Stephen Salter on the development of instrumentation, absorbing wave-makers, and multi-directional wave tanks for the development of the Duck wave energy device.

Professor David Ingram holds a personal chair in computational fluid dynamics in the Institute for Energy Systems. His personal research interests include the development of computational fluid dynamics models for highly transient, free surface flows, and wave breaking and impact on structures.

BEST PRACTICE GUIDELINES FOR TANK TESTING OF WAVE ENERGY CONVERTERS

Grégory S. Payne, Jamie R.M. Taylor, and David Ingram
University of Edinburgh, Edinburgh, United Kingdom
www.ed.ac.uk

ABSTRACT

Experimental tank testing is a key aspect of wave energy conversion research. The performance of designs can be assessed in an accessible and controlled environment and at a fraction of the cost of sea trials.

Wave energy converter (WEC) tank testing is complex and has its own specificities compared with model testing of ships and offshore structures. This largely reflects the fact that the main quantity of interest is wave energy: how much is available and how much is harvested by the model.

This paper provides an extensive overview of the various aspects of WEC tank testing. These are divided into three categories: physical model, measurements, and wave generation. For each of them, current best practice guidelines are given.

KEY WORDS

Wave energy, tank testing, wave generation

NOMENCLATURE

BDM	=	Bayesian directional method	MLM	=	maximum likelihood method
CFD	=	Computational fluid dynamics	NWT	=	numerical wave tank
DFT	=	discrete Fourier transform	OWC	=	oscillating water column
DSF	=	directional spreading function	PTO	=	power take-off
FFT	=	fast Fourier transform	WEC	=	wave energy converter
IDFT	=	inverse discrete Fourier transform			
LES	=	large eddy simulation			

INTRODUCTION

The primary reason for the tank testing of wave energy converters (WECs) is to enable an investigation of the general principals governing the behaviour of the WEC under controlled conditions. Such tests are commonly used to investigate the impact of different configurations, dimensions, and other key design parameters of the WEC influencing its predicted performance and survivability characteristics. Furthermore it is normal for a wide range of tests to be conducted at these earlier stages, leading to better understanding of the influence of critical parameters and improving theoretical models of performance. Even at small scales, the controlled laboratory environment allows the performance of the WEC in rare (e.g. 100 year) sea conditions to be tested repeatedly and for the impact of modifications to the WEC to be examined in identical sea conditions. Not only is the test environment accessible, controlled, and repeatable, but also the cost of tank testing is a small fraction of that of sea trials. This is an advantage that led to Stephen Salter's well known comment: "It is much better to discover one's design mistakes at a small scale" [Salter et al., 2006].

Figure 1 shows a typical tank test of a WEC and illustrates the key aspects of a laboratory test, namely the model, the measurement systems, and the wave makers.

Entering the laboratory not only permits access to a controlled and repeatable environment, but also allows the use of measurement techniques that cannot be applied in the field. For example, optical systems can be deployed for measuring the motion of the WEC (using stereoscopic infra-red cameras, see "*Sensors*" on page 47). These advantages are offset by the fact that real (prototype) power take-offs (PTOs), control and mooring systems cannot, normally, be scaled down to laboratory scale and must be modeled in some way. This differentiates the scale testing of WECs from the model testing of ships and offshore structures, and has led to the development of specialist laboratories and centres of excellence around the world.

The current drive to develop commercial WECs has led to the identification of a number of barriers to full commercialization. The 2006 report for the International Energy Agency [AEA Energy and Environment, 2006] implementing agreement on ocean energy states that "the comparison of different technologies is made difficult by the absence of internationally recognized standards for development, testing, and measurement." The IEA report, together with national initiatives (including UK Energy Research Centre's Marine Technology Roadmap [Mueller and Jeffrey, 2008]), has led to a number of initiatives to develop best practice protocols for the experimental testing of wave energy converters. The International Electrotechnical Commission has established technical committee TC114 to develop standards for ocean energy converters, and the European Commission has funded the 7th Framework program, EquiMar project (FP7-213380) on "Equitable Testing and Evaluation of Marine Energy Extraction Devices in terms of Performance, Cost, and Environmental Impact."

The UK Engineering and Physical Sciences Research Council's SuperGen Marine project (EP/E040136) is a consortium project led

Figure 1: Tank testing experiments carried out in the Edinburgh curved tank show key aspects of experimental practice. 1(a): 100th scale Sloped IPS buoy in mixed seas. 1(b): comparison between two types of wave gauge.

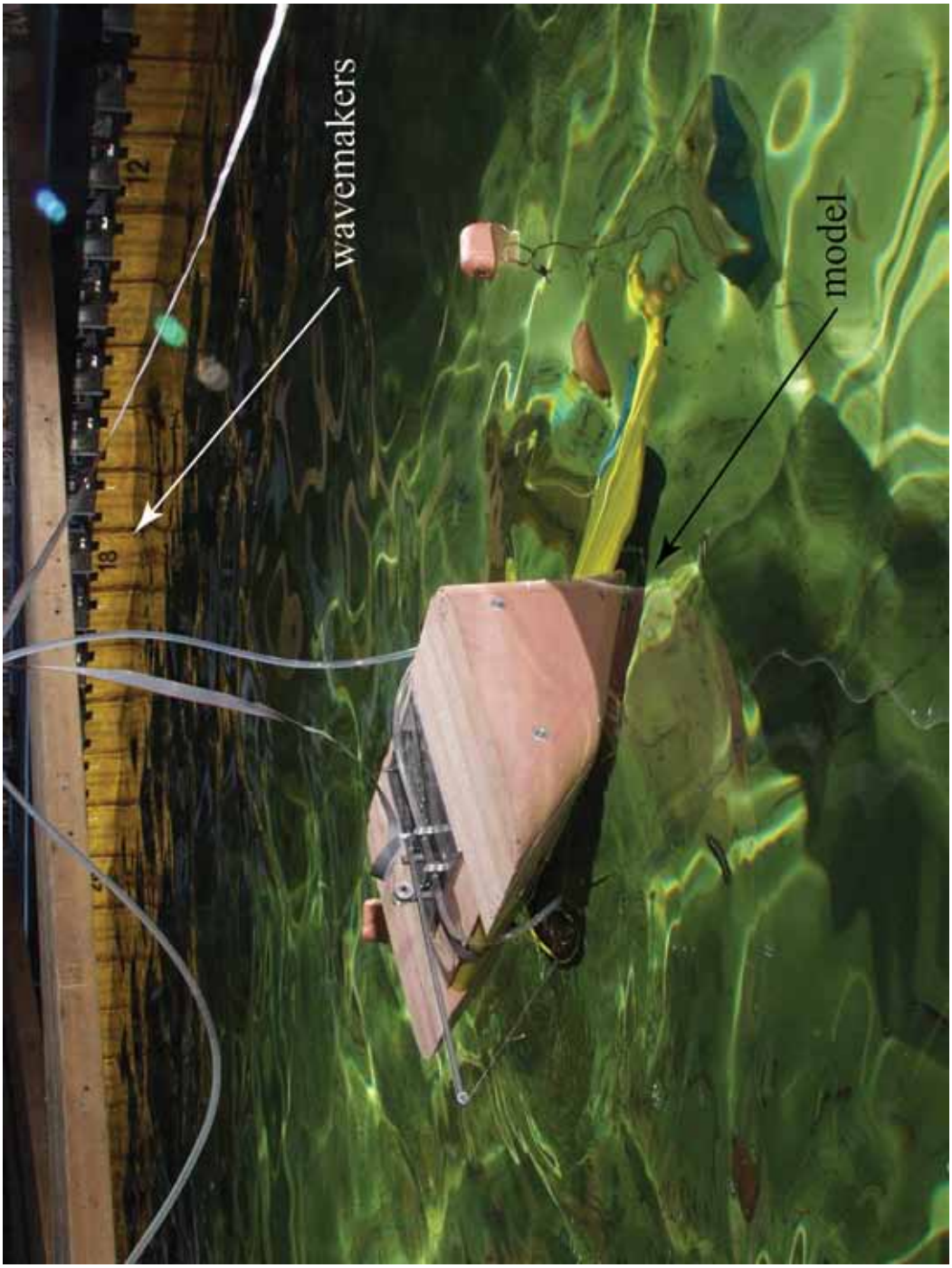

Figure 1(a)

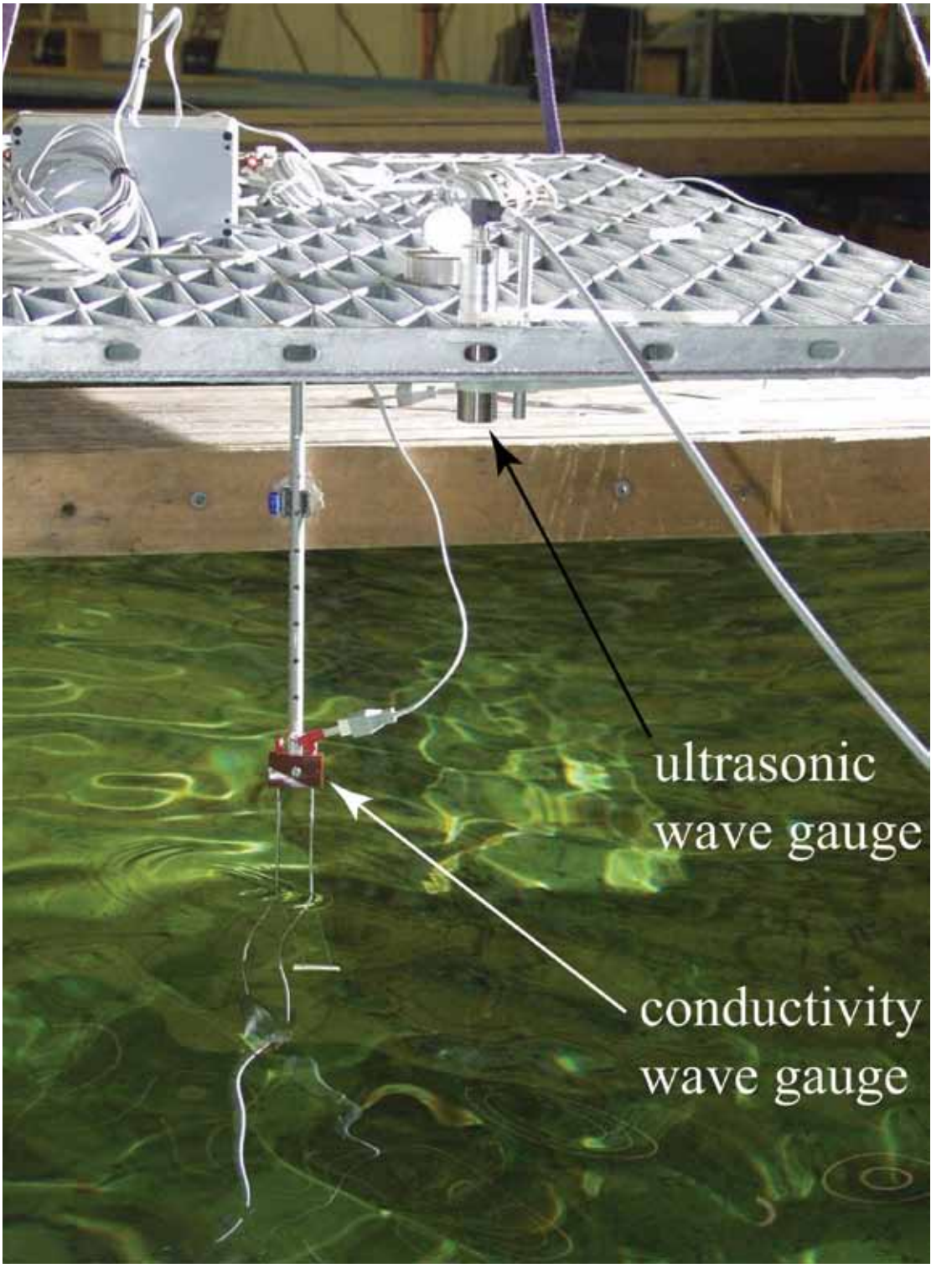

Figure 1(b)

by the University of Edinburgh involving leading research groups across five universities (Edinburgh, Heriot-Watt, Lancaster, Strathclyde, and Queen's Belfast). Work stream 1 is concerned with the convergence of physical testing and numerical modeling of WEC concepts. SuperGen is seeking to ensure that comparable results can be obtained in any of the wave tanks available within the consortium.

These national and international efforts are not independent of each other, since consortium members are involved with the national mirror committees for TC114, and are participating in the EquiMar project. Indeed, it is critical that best practice guidance is based on a broad consensus of opinion if it is to be adopted by both established and new experimental facilities and ultimately incorporated into international standards.

To this end, SuperGen has produced a best practice guide drawing on both expertise within the consortium and published literature. In this paper, the authors have summarized the key sections of the guide, which cover the physical model, measurement, wave generation (both deterministic and nondeterministic approaches), tank calibration, and phase locking.

PHYSICAL MODEL

A physical model is used in a wave tank to investigate at scale the behaviour of a wave energy converter concept. In most cases, some aspects of the full-scale device are simplified in the scaled model. For the power take-off system, an electromagnetic damper might, for example, be used in place of the full-scale hydraulic system. Model tank tests are typically used to investigate the following points:

- Power capture characteristics
- Hydrodynamics
- Power take-off principle and associated control
- Moorings

This section introduces the issue of scaling and its specific impact on model testing of WECs. It then focuses on power take-off modeling and sensors.

Scaling

Generally speaking, in the mechanical interactions between fluids and solids, three kinds of forces are of comparable importance. These are associated with inertia F_i, gravitation F_g, and viscosity F_v.

$$F_i \propto \rho U^2 l^2 \quad (1)$$

$$F_g \propto \rho g l^3 \quad (2)$$

$$F_v \propto \mu U l \quad (3)$$

where U is the fluid velocity, g the gravitational acceleration, l the length characterizing fluid/solid interaction phenomenon, and μ is the dynamic viscosity.

Depending on the phenomenon investigated, the relative magnitude of those forces varies. It is useful to quantify their relative importance. This is typically done using two non-dimensional quantities: the Froude number Fr and the Reynolds number Re.

$$Fr = \frac{U}{\sqrt{gl}} \propto \frac{F_i}{F_g} \propto \frac{\text{inertial force}}{\text{gravitational force}} \quad (4)$$

$$Re = \frac{Ul}{\nu} \propto \frac{F_i}{F_v} \propto \frac{\text{inertial force}}{\text{viscous force}} \quad (5)$$

where v is the kinematic viscosity $(v = \mu/\rho)$.

Ideally, when designing scaled model testing, it is desirable to retain the same balance between inertial, gravitational, and viscous effects as that of the full-scale phenomenon. This implies ensuring that the values of both *Fr* and *Re* at model-scale are the same as the full-scale ones. In practice, this is usually difficult to achieve, especially at small scale. As an example, consider the investigation of the forward motion of a ship using a 1/100th scale model in a towing tank. Assuming that the gravitational acceleration *g* is the same in both model and full-scale conditions, if *Fr* is to be kept constant, according to (4), the value of the forward speed *U*, at model-scale has to be 1/10th of the full-scale one. Now assuming that the fluid used with the model is the same as in full-scale, *v* is the same in both model and full-scale conditions. If *Re* is to be kept constant, according to (5), the value of *U* at model-scale has to be 100 times that of the full-scale value. The obvious way to overcome these conflicting requirements would be to increase *g* and/or decrease *v*. This would involve running the model experiments in a centrifuge and/or using fluids whose viscosities are lower than that of the full-scale one. Unfortunately, this kind of experimental set up is not practical for tank testing of wave energy devices, where tanks are too large to fit in centrifuges and are filled with water.

During the interaction between waves and solid bodies, the effects of viscosity are generally felt in the boundary layer, in the close vicinity of the water-body interface. In the rest of the fluid volume, viscous effects are generally negligible. The relative influence of viscous forces will thus be greater for complex WEC geometries that have large wetted-surface areas in relation to their immersed volumes compared with more compact WEC shapes that have lower ratios of wetted-area to volume. For many tank-scale WECs, the net influence of viscous forces on body motions is small and Froude scaling can be assumed to be satisfied. This assumption that the ratio of inertial forces to gravitational forces is the same at model-scale and at full-scale generally leads to conservative predictions of full-scale device behaviour. A good introduction to the very important topic of scale can be found in chapters 1 and 2 of Newman [1977].

Practical implications of Froude scaling on power take-off modeling

For wave energy applications, one of the key consequences of Froude scaling is the scaling law of wave power.

Let *s* be the geometric scale between model and full-scale conditions. From (4), if *Fr* and *g* are constant, then *U* scales with $\sqrt{s}$. In terms of dimensions:

$$[U] = \frac{[L]}{[T]} \tag{6}$$

where *U*, *L*, and *T* are the dimensions of velocity, length, and time, respectively. So time scales also with $\sqrt{s}$. It can be noted that this result can also be derived from the dispersion relation of gravity waves. For the sake of simplicity, consider the deep water case. The dispersion relation yields:

$$\lambda = \frac{gT^2}{2\pi} \tag{7}$$

where λ is the wavelength and *T* the wave period (derivation of (7) can be found in Sarpkaya and Isaacson [1981]). *g* is the same

for both full scale and model conditions, so (7) is true in both cases. Therefore, *T* scales with $\sqrt{s}$.

The dimensions of power are:

$$[P] = \frac{[M][L]^2}{[T]^3} \quad (8)$$

where *M* is the dimension of mass. As mass is proportional to volume, *M* scales with s^3, and thus, power scales with $s^{3.5}$.

Depending on the size of the models and tanks used, the model scales are typically of the order of 1/30th to 1/100th. Assuming a full-scale power take-off rated at 1 MW, the model power rating would be of the order of 0.1 to 7 W. This means that in order to simulate full-scale behaviour accurately, power dissipation due to friction losses in the model power take-off should be kept very low, ideally, down to the 'milliwatt' level for the smaller scale models. It is, therefore, important to design models with very low friction bearing between moving parts. Hydrostatic bearings have very low friction but tend to be more complex to implement than bush or ball bearings. Taylor and Mackay [2001] have successfully used water fed hydrostatic bearings on a model power take-off. Further information on hydrostatic bearings can be found in Stansfield [1970].

Froude scaling overview

Using the same reasoning as in *"Practical implications of Froude scaling on power take-off modeling"* (page 44), the scaling of various quantities of interest can be derived. Some of these are shown in Table 1.

Quantity	Scaling
wave height and length	s
wave period	$s^{0.5}$
wave frequency	$s^{-0.5}$
power density	$s^{2.5}$
linear displacement	s
angular displacement	1
linear velocity	$s^{0.5}$
angular velocity	$s^{-0.5}$
linear acceleration	1
angular acceleration	s^{-1}
mass	s^3
force	s^3
torque	s^4
power	$s^{3.5}$
linear stiffness	s^2
angular stiffness	s^4
linear damping	$s^{2.5}$
angular damping	$s^{4.5}$

Table 1: Froude scaling law for various quantities. *s* is the geometric scale. When the scaling is 1, it means that the value of the quantity is not affected by scale. The term "power density" refers to power per unit length.

Scale issues with oscillating water column devices

In oscillating water column (OWC) wave energy converters, the displacement of the water column is driven by hydrodynamic effects. The power take-off mechanism relies on aerodynamics as the air in the OWC chamber is forced back and forth through a turbine. This combination of hydrodynamics

and aerodynamics renders scaling considerations for OWCs more complex than standard Froudean scaling.

The hydrodynamics interactions between waves and the OWC are dominated by inertial and gravitational forces. The aerodynamics of the air volume of the OWC chamber is dominated by the compression force F_c. Assuming volume deformation of the chamber in one dimension and reversible and adiabatic conditions:

$$F_c \propto P_0 \kappa l^2 \tag{9}$$

where P_0 is the initial air pressure, κ the isentropic exponent, and l the characteristic length [Weber, 2007]. Both inertia and pressure forces act as restoring forces in the heaving motion of the water column. Maintaining the same balance between these two at model and full-scale involves keeping the ratio:

$$\frac{F_i}{F_c} \propto \frac{\rho U^2}{P_0 \kappa} \tag{10}$$

constant. From (10) and (4), keeping both the F_i / F_c ratio and the Froude number constant involves keeping the ratio:

$$\frac{\rho g l}{P_0 \kappa} \tag{11}$$

constant which is difficult in practice. One approach to address this issue is to design a model with different scales above and below the waterline. In other words, the horizontal cross section of the chamber remains the same, but the top part of the chamber can be made higher to increase its volume. This has been tried by Maunsell and Murphy [2005]. More information on the topic of OWC scaling can be found in Weber [2007] on which this treatment is based.

Power Take-Off System

Scale modeling of power take-off mechanisms is not straight forward. The technologies suitable for full-scale devices usually do not lend themselves to down-scaling. This is mainly due to the scaling factor of power in Froude scaling (see *"Practical implications of Froude scaling on power take-off modeling"* on page 44). This is the case for hydraulic rams, which are an attractive first stage for full-scale power-offs but whose friction losses make them unsuitable for scaled models.

The ideal model power take-off dynamometer provides a means of applying arbitrarily defined forces between the wave-driven and the reactive body-elements of the WEC. It is convenient if the forces can be accurately varied as linear functions of a control voltage or current. The system should have as few additional mechanical artifacts as possible. For example, friction losses and mechanical backlash should be minimized. Typically, to represent pure damping, the force provided by the dynamometer will be configured to be proportional to the relative velocity of the wave-driven motions of the WEC body elements and will act in opposition to them. In order to explore maximum power-capture techniques, there should be few limitations on the kind of control algorithm that can be implemented. Where it is possible to use them, amplifier-driven DC electric-motors provide the best means for implementing this kind of control. The best kind of DC motor is the brushless type as made by Aeroflex – although their limited angular range may be unsuitable for many models. DC motor force is directly

proportional to current, so current-amplifiers should be used. For accurate results (unless a brushless motor is used), some means of measuring the motor force may be required. Typically this will involve the incorporation of strain-gauged components in the force path. The flexibility offered by these kinds of dynamometer systems often makes it possible to drive the WEC in calm water in order to measure and calculate its hydrodynamic coefficients – the added mass and the radiation damping.

Some mechanical dampers can be calibrated with reasonable accuracy. They can then be implemented in model power take-offs to carry out quantitative measurements. It should be noted, however, that when using this method, the resisting force applied to the prime mover cannot be controlled with the same freedom as with DC motors. Moreover, that force is often not fully linear with the prime mover displacement or velocity. In the case of OWC, an equivalent approach relies on aerodynamic dampers. These are typically carpet sheets or slit shims whose flow to pressure characteristics can be calibrated [Lucas et al., 2007]. Experimenters should be aware that carpet characteristics are affected by the moisture level of the carpet.

Cruder power take-offs can also be used. This depends on the stage of investigation considered. For early experimental tests, one might only be interested in qualitative assessments of the impact of the power take-off resistance to the prime mover on the model behaviour. In this case, some kind of simple friction-brake may be suitable.

It is important to emphasize that the quality of the model power take-off affects directly the range and the quality of the measurements that can be carried out. The technology chosen should, therefore, be appropriate to the scope of the model testing investigation.

Sensors

Sensors and transducers should interfere as little as possible with the behaviour of the models that they are measuring. In many cases, video motion tracking devices such as those manufactured by Qualisys AB have made "motion capture" relatively easy and generally only require the attachment of lightweight optical markers to the model. These systems can, however, only record "external" motions of the model and other types of sensors are often needed to measure other physical quantities or internal motions of the power take-off.

Sensor implementation

Motion, velocity, and force sensors should generally be fitted as closely as possible to the physical phenomenon they are intended to measure. The idea is to avoid corrupting the measurements with mechanical artifacts (such as backlash or excessive friction) from linkages or bearings. Force measurement usually involves the inclusion into the force path of compliant elements whose dimensional changes are captured by strain-gauges or piezo crystals. The effect of the compliance is usually to lower the natural frequency of the system of which the sensor forms a part. Where the force signal is part of a force feedback loop, as might be the case with a power take-off dynamometer, care must be taken to keep the force path mechanically stiff so that resonances are well above the tank wave frequency band. Otherwise, it may be difficult to make the system stable.

Signal processing

When putting together a data acquisition system to log measurements from sensors, the aim is always to get as much "signal" and as little "noise" as possible.

Most electrical noise is at frequencies that are very much higher than tank wave frequencies and is reasonably easy to eliminate by the careful use of low-pass filters (Horowitz and Hill, 1989]. However, in the design of electronic instrumentation, one also has to be very careful not to pick up some dangerously close to 50 or 60 Hz noise from nearby mains-operated electrical equipment. It must be ensured that the design of the instruments eliminates this. An important rule is to never start serious data acquisition until having checked the signal quality and the comparative amount of "signal to noise." There is only one way to do this, and that is to look at each signal on an oscilloscope whilst the wave and model systems are running at the lowest wave amplitudes that will be used during experiments. The dynamic range of all of the signals relative to the full-scale range of the data acquisition system should also be checked. Ideally, to get the best resolution, all incoming signals at maximum value will reach at least two-thirds of the data acquisition maximum. It is also important to keep checking the signal quality during experiments in case any sensor fails or starts to get wet.

Convention dictates that signals that are to be sampled by a data acquisition system should first be passed through a low-pass filter. Without such filtering, signal components at frequencies greater than half of the data sampling frequency break through into the sampled signal band as "aliasing" (see *"Aliasing"* on page 49). However, it is likely that one will not always be using the same data sampling frequency so it may be difficult to decide on the best filter cutoff frequency. For long experiments, it might suffice to sample at twice the frequency of the shortest wave component. In another experiment, one might want to look at the transient effects of a breaking wave and to, therefore, sample at a much higher rate – perhaps up to several hundred hertz.

If the signals are very clean, one might not need to use any low-pass filtering. A more conservative approach is to "roll-off all signals at a frequency around 1 kHz with first-order low-pass filters." These will have little effect on the phases of the much lower frequency wave signals. In any event, after sampling any such phase errors could be subsequently corrected in the frequency domain.

MEASUREMENT

The quantities which are of interest to measure in the context of tank testing for wave energy applications are numerous. This section provides guidelines on the generic aspects of tank measurement and focuses on wave measurements, from hardware to methods for estimating wave fields.

Measurements in the Context of Fourier Analysis

Frequency analysis is a widely used technique for investigating phenomena involving water waves. The general idea of Fourier analysis is based on the fact that a periodic function f of period T can be expressed as the sum of its harmonic components:

$$f(t) = a_0 + \sum_{k=1}^{\infty} \left(a_k \cos \frac{2\pi kt}{T} + b_k \sin \frac{2\pi kt}{T} \right) \quad (12)$$

where the a_k and b_k are the Fourier coefficients defined by:

$$a_0 = \frac{1}{T} \int_{-T/2}^{T/2} f(t)dt \quad (13)$$

$$a_k = \frac{2}{T} \int_{-T/2}^{T/2} f(t) \cos \frac{2\pi kt}{T} dt \quad \text{for} \quad k \geq 1$$

$$b_k = \frac{2}{T} \int_{-T/2}^{T/2} f(t) \sin \frac{2\pi kt}{T} dt \quad \text{for} \quad k \geq 1$$

By looking at the amplitude of the coefficients, one can assess the spectral content of the signal. More information on this topic can be found in Newland [2005].

The method commonly used to carry out a spectral analysis of a discrete time series x_p of N samples ($p = 0, 1, 2, ..., N - 1$) is the Discrete Fourier Transform (DFT) which is defined, using complex notation, as follows:

$$X_k = \frac{1}{N} \sum_{p=0}^{N-1} x_p e^{-i\frac{2\pi kp}{N}} \quad \text{for} \quad k = 0, 1, \ldots, N-1 \quad (14)$$

The Inverse Discrete Fourier Transform is given by:

$$x_p = \sum_{k=0}^{N-1} X_k e^{i\frac{2\pi kp}{N}} \quad \text{for} \quad p = 0, 1, \ldots, N-1 \quad (15)$$

The DFT is a practical method to estimate the spectrum of a continuous time series. However, it should be borne in mind that the DFT does not output the true continuous spectrum but an estimate of it. The quality of the estimate is directly influenced by the way the continuous time series is sampled.

Aliasing

The sampling frequency used to sample a continuous time series dictates the frequency range and impacts on the quality of the spectrum calculated by the DFT. One should ensure that the sampling frequency is at least twice that of the highest frequency component of the time series.

When sampling at frequency f_s the DFT process is unable to distinguish between components whose frequencies f_1 and f_2 are symmetrical with respect to $f_s/2$: $f_1 \leq f_s/2$ and $f_2 = f_s - f_1$. Figure 2 illustrates this phenomenon. It shows two sine waves, one of frequency 0.5 Hz and the other of 3.5 Hz. The circles represent the sampled data with a sampling frequency of 4 Hz. The 3.5 Hz sine wave has deliberately been shifted by 180°.

It can be seen that the sampled values are the same for the 0.5 Hz and the 3.5 Hz sin waves.

In the DFT output, the sum of the measured amplitudes of the two components ends up being equally split between the two frequency components (f_1 and f_2) even if their true respective amplitudes are different. The outcome is a spectrum symmetrical with respect to $f_s/2$. If the true amplitude of component f_2 is zero, the DFT will output a spectrum with components at frequencies f_1 and f_2 whose amplitudes are equal to half the true amplitude of component f_1. By doubling the amplitude of DFT component f_1 and discarding DFT components of frequency above $f_s/2$, the true spectrum can be derived. This is, however, not possible when the amplitude of the true component f_2 is not zero. In this case, the spectrum obtained is distorted and does not suitably approximate

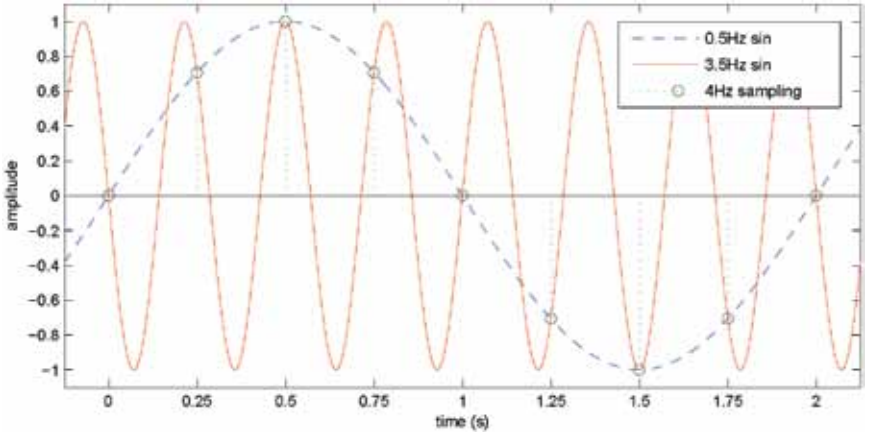

Figure 2: Example of aliasing.

the true spectrum. This can be generalized for any numbers of frequency components. The phenomenon is called "aliasing" and $f_s/2$ is referred to as the "Nyquist frequency" or sometimes the "folding frequency." More detail on that topic can be found page 118 of Newland [2005].

To summarize, the sampling frequency has to be chosen so that the Nyquist frequency is above the frequencies of *all* the components of the time series and not only of the ones of interest. A practical way to achieve this is to use an appropriate low-pass filter before sampling the signal.

Frequency resolution

The frequency resolution of the DFT is determined by the sampling duration. To be more specific, in the DFT process, the time series is correlated with sinusoids whose frequencies are integer multiples of the inverse of the sampling duration. In other words, if the time series is sampled for a duration ΔT_{dur} it will be correlated with sinusoids of frequency:

$$f_k = \frac{k}{\Delta T_{dur}} \quad \text{with} \quad k = 0, 1, \ldots, N-1 \tag{16}$$

where N is the total number of samples. The frequency resolution of the DFT is therefore $1/\Delta T_{dur}$.

Let us consider a time series that consists of a single sinusoid of frequency f_i. If the sampling duration is chosen so that f_i does not correspond to any of the frequencies of the correlation sinusoids (that is if $f_i \neq f_k$ with $k = 0, 1, ..., N-1$), then the amplitude of the true component will be spread over the nearest DFT components. This phenomenon is commonly referred to as "spilling." This is illustrated in Figure 3 where the time series is a sinusoid of amplitude 1 and frequency 31/32 Hz. The sample frequency is 32 Hz and the sampling duration is 16s. It should noted that for clarity consideration, the spectrum is truncated and does not display the whole frequency range of the DFT.

When the sampling duration is such that one of the f_k matches f_i, the resulting spectrum is much "cleaner." This is shown in Figure 4 where the parameters are the same as for Figure 3 except for the sampling duration which is here 32s.

In order to obtain good quality spectra from DFT, it is recommended to choose a sampling frequency and a sampling duration so that the frequency of each component of the time series analyzed is matched by one of the f_k. When the time series is derived from a true natural process, like wave elevation at one point in the ocean, this is not possible because there will be an infinite number of frequency components. In a wave tank, however, the command signal sent to the wave makers is usually computed by Inverse Discrete Fourier Transform (IDFT) (see "*Wave generation*" on page 59) and therefore contains only a finite number of frequency components which can be matched by the f_k.

Periodicity of the signal

Theoretically speaking, the DFT performs better if the time series analyzed is periodic and if the sampling duration corresponds to an integer multiple of the period. If the wave generation system of the tank is controlled in a deterministic manner (see *"The deterministic approach"* on page 60), the sampling duration should be chosen so that it corresponds to an integer multiple of the pseudo period or repeat time of the system. If the signal sampled is not periodic, it is recommended to use a tapered data window to smooth the data at both ends of the sampled time series before carrying out the DFT. A data tapered window is basically a weighing function which gives more importance to the middle of the time series compared to the extremities. It can be seen as "making" the time series "look" more periodic by smoothly bringing the values of both ends to zero. This process is illustrated in Figure 5 where a cosine tapered window is applied to the time series of a random signal. It should be noted that periodicity "enforcing" by data windowing is done at the cost of distorting data. More information on this topic can be found in chapter 11 of Newland [2005].

Fast Fourier Transform

The name Fast Fourier Transform (FFT) refers to an algorithm used to compute the DFT. It was originally introduced by Cooley and Tukey [1965]. It is particularly computationally efficient and accurate. It has now become the standard method for deriving the DFT. There are several variations of the FFT algorithm but the most common ones require the number of samples N to be a power of 2. If it is not the case, most algorithms extend the number of samples to reach the nearest power of 2 by "adding" zeros at the end of the original time series. This results in a spilling phenomenon.

Wave Measurement Hardware

There are several types of wave gauges used to measure waves in wave basins. Here is a brief overview of the technologies available.

Float gauge

This technique relies on measuring the vertical displacement of a float following the water surface. Sub-millimetre accuracy has been achieved with this method (see chapter 4 of Nebel [1994]). To avoid following errors, the heave motion of the float should be as close as possible to the vertical motion of water particles. This is achieved by ensuring that the ratio of the float water plan area over the float inertia is as high as possible. The idea is to make sure that the natural frequency of the float in heave is much higher than the frequency of the measured waves. A description of a gauge of this type developed at the University of Edinburgh can be found on page 24.4 of Jeffrey et al. [1976].

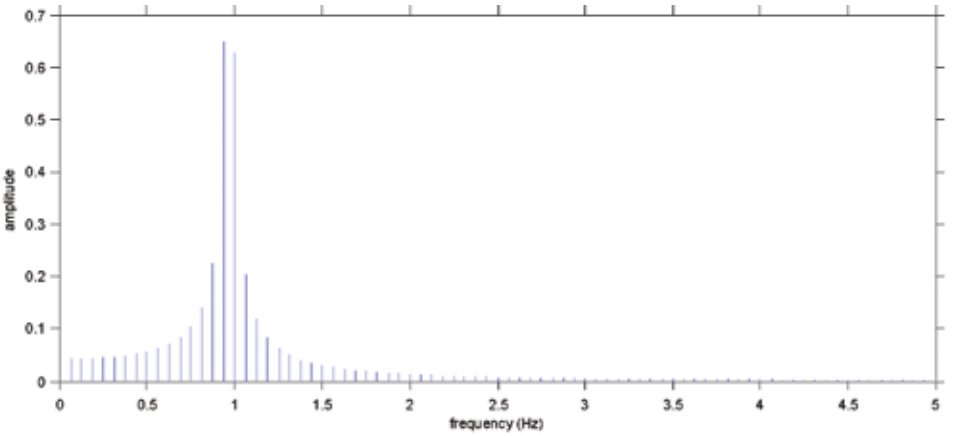

Figure 3: Spectrum exhibiting spilling due to inappropriate sampling duration (31/32 Hz signal sampled for 16s at 32 Hz).

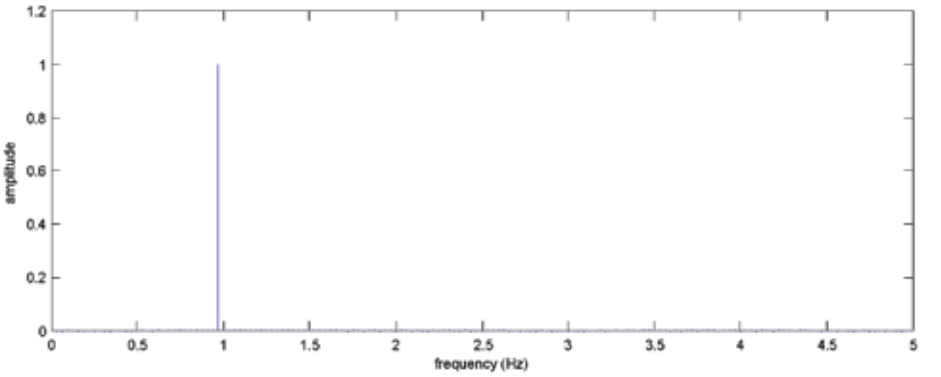

Figure 4: Spectrum without spilling (31/32 Hz signal sampled for 32s at 32 Hz).

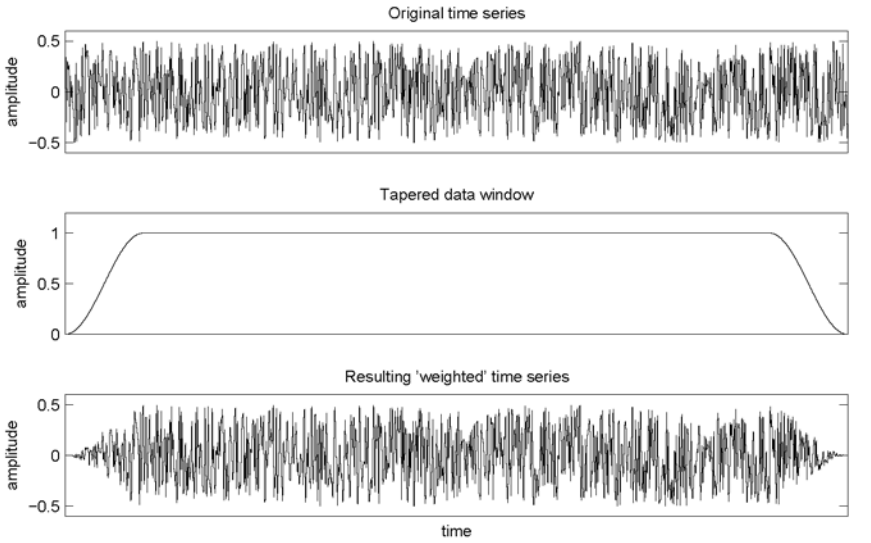

Figure 5: Application of a tapered window to a random signal.

Capacitance gauge
Wave gauges of this type typically consist of two vertical metal rods partly immersed. One or both of the rods is covered with a thin layer of electrical insulator. The capacitance measured between the two rods is linearly dependant on the immersion depth. Alternatively, the non insulated electrode can be taken away and replaced by the tank electrical ground. More information on capacitance wave gauge working principle can be found in Clayson [1989].

The advantage of this technology is that calibration is fairly stable with time. On the other hand, the insulation layer on the rods can be a source of reliability issues. In order to achieve reasonably high capacitance values, the insulation coating has to be very thin and it can, therefore, be easily damaged.

Water surface following gauge
This technology relies on a servo-drive mechanical system tracking the water surface. It provides an absolute measurement of the water level and is calibration-free.

A prototype of this type of gauge has been built at the University of Edinburgh using a capacitive sensor to detect the water surface. 0.5 mm accuracy has been achieved. More information can be found in Spinneken [2004].

Ultrasound gauge
These sensors, such as those made by Nortek, beam high-frequency sound vertically downwards. Some of the beam is reflected back by the moving water surface and the wave height is derived from the corresponding time-of-flight. This measurement is inversely proportional to the speed of sound in air, which is sensitive to temperature and humidity and so calibration needs to be carried out regularly. An immersed three-degree-of-freedom ultrasound wave measuring system was built by Rogers [1987]. It used an active float-based piezo "pinger" and an array of three acoustic receivers on the tank floor.

Conductive wave gauges
Conductive wave gauges typically consist of two thin, parallel vertical metal rods partly immersed. The water height is derived from the conductivity between the rods, which increases with the immersion of the rods. More information can be found in Clayson [1989].

Regular calibration is required as the water conductivity changes. In Thompson and Long [1987], it is stated that at the United States Army Engineer Waterways Experiment Station, wave gauges are calibrated statically at least twice a day.

It also states that, ideally, the calibration should be dynamic but that given the complexity of this procedure, most laboratories rely on static calibration. It is recommended to run waves in the tank for a few minutes before calibrating the gauges in order to mix the water to make the conductivity the same everywhere in the tank.

Optical gauge
This technique relies on the principle of triangulation. A spot created by the scattering of laser light at the water surface is detected by an off-axis camera. The images from the camera are processed to derive the centroid of the spot. The centroid position is transformed into a height value using a polynomial best-fit function established by calibration. This is

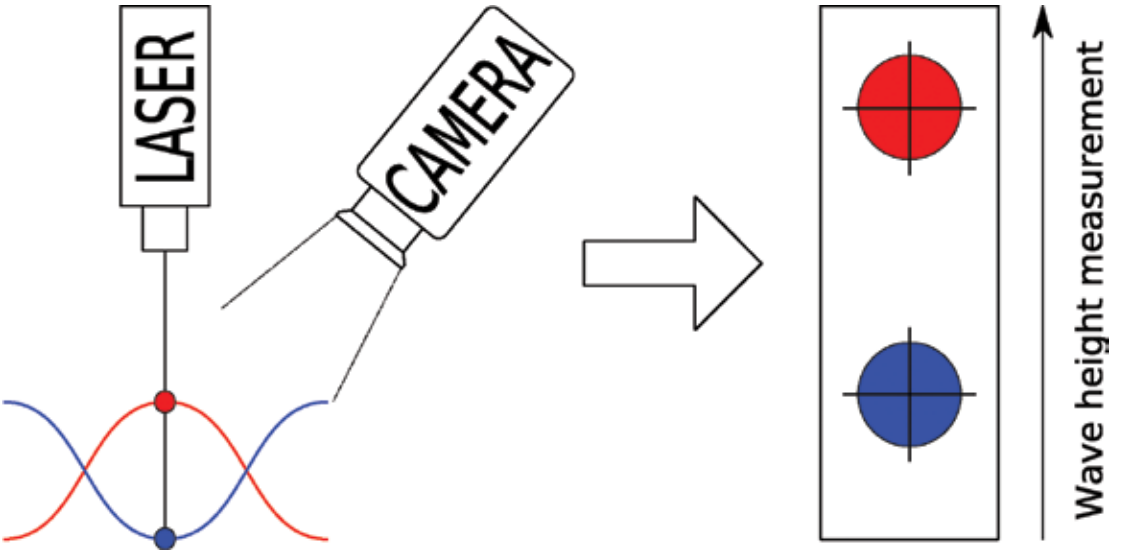

Figure 6: Schematic of an optical wave gauge.

summarized in Figure 6 where height measurements are shown for a wave crest (in red) and a trough (in blue).

Optical gauges are non-contact so the measurements are not biased by surface tension as in capacitive and conductive wave gauges which suffer from meniscus effect. Optical sensing allows adjustable resolution by choice of the camera optics magnification. Sub-millimetre accuracies have been achieved on waves with more than 1000 mm peak to trough height. The calibration of such gauges is straightforward and stable.

Two-Dimensional Wave Reflection

In a bounded fluid domain such as a wave tank or a wave flume, wave reflections from the boundaries of the basin are unavoidable. Moreover, the presence of a model in the tank will also lead to wave reflections. It is, therefore, important to work out the incident and reflected wave parameters.

An early method, which can only be used with regular waves, consists in placing two wave probes aligned with the direction of propagation of the waves and a quarter of the wavelength apart. While maintaining constant distance between the two probes, they are translated along the wave propagation direction until one is located at a node and the other one at an antinode of the standing wave pattern created by the reflection. This is easy to do if the gauges are properly calibrated and if a real-time signal proportional to the difference in wave heights at the two gauges is visibly displayed. Averaging the signal between the two probes yields the incident wave amplitude. Dividing by two the difference between the two probes signal yields the reflected wave amplitude.

The above method is most practical in narrow wave tanks. It is restricted to regular waves and prior knowledge of the wavelength is required. A large body of work on more versatile methods for 2-D wave reflection analysis is

reported in the literature. This comes mainly from the field of coastal engineering.

Wave elevations are recorded simultaneously at a number of locations (at least two) in a line parallel to the direction of propagation of the waves, with a known spacing between the wave probes.

A Fourier transform is then applied to the time series to derive the different frequency components of the wave field. For each of these, the parameters of the incident and reflected waves are computed. When working with regular waves, the Fourier transform is generally used to find out the fundamental frequency of the wave.

Various methods are then available to compute the incident and reflected wave parameters.

The Goda and Suzuki method

The earliest and simplest technique is described in Thornton and Calhoun [1972] and Goda and Suzuki [1976] and is often referred to as the Goda and Suzuki method. It involves only two measuring locations. For a regular wave, it assumes that the wave elevation measured at each probe is the sum of two sinusoids of the same frequency travelling in opposite directions. The method yields the amplitude of the incident and reflected waves as well as the phase shift between the two. Details on the implementation of the method can be found in Goda and Suzuki [1976] for random wave applications and in Isaacson [1991] for the case of regular waves. It is important to point out that the method exhibits singularities when the probe spacing is equal to an integer number of half wave lengths. It is, therefore, recommended to avoid the vicinity of the singularities. This is, unfortunately, not always possible when analyzing reflections in random waves, especially with a wide spectrum range. A compromise needs, therefore, to be made which usually involves giving higher weighings to the frequency bands of interest, around the peak frequencies, for example. More details on the range of application of this method can be found in the two previously cited references.

The Mansard and Funke method

The Mansard and Funke method [Mansard and Funke, 1980] is the most commonly used. It uses three wave probes and can be considered as an improvement of the Goda and Suzuki approach. As for the latter, sinusoids are fitted to the incident and reflected waves, but the data from the extra probe makes it possible to minimize the squared error between the outcome of the fittings and the measured wave elevations. The main advantage of this method is to make the wave reflection analysis less sensitive to the noise contaminating the measurements [Isaacson, 1991]. As with the previous approach, the Mansard and Funke method exhibits singularities. If the three probes are equidistant, the method breaks down when the spacing between two adjacent probes is an integer number of half wave lengths as for the previous method. If the probes are not equidistant, the conditions of occurrence of the singularities are more complex and can be found in Isaacson [1991] and Mansard and Funke [1980].

Discussion

In Isaacson [1991], the author presents a comparative study of the two above methods for regular waves. He carries out a sensitivity analysis on the accuracy of the incident and reflected wave parameters to errors on the

measured wave elevations. The Mansard and Funke is found to be the most accurate.

It is important to point out that the two methods are based on linear dispersion theory. In other words, they assume that the incident and reflected waves are perfect sinusoids, which is not the case in reality. This is illustrated in Mansard and Funke [1987] where the authors report that for regular waves, the incident and reflected wave heights estimated by their method are too small compared to the wave heights derived from zero crossing analysis. The process of fitting sinusoids to the wave field discards the bound harmonics from the analysis whereas the wave height computation relying on a zero crossing approach does not.

Multidirectional Wave Spectra

When analyzing the performance of a wave energy converter model in a directional wave tank, it is important to estimate as accurately as possible the incident wave conditions to which the model is exposed.

Many techniques for deriving directional characteristics of wave fields are reported in the literature. Most of them were developed by oceanographers to measure waves in the real seas. Benoit et al. [1997] give a good overview of those different techniques and the present section will broadly follow this paper.

The dependency of the energy spectrum on frequency and direction is described by the energy spectrum $E(\omega, \theta)$, which is a function of the wave angular frequency ω and of the wave direction of propagation θ. E is an energy per unit sea surface, per unit frequency, and per unit angle. The unit of E is, therefore, $J.m^{-2}.Hz^{-1}.rad^{-1}$ but is sometime expressed as $N.m^{-1}.Hz^{-1}.rad^{-1}$.

It is also common to analyze a wave field in terms of directional variance spectrum $S(\omega, \theta)$. This corresponds to the variance of the wave elevation which is proportional to the wave energy:

$$S(\omega,\theta) = \frac{E(\omega,\theta)}{\rho g} \tag{17}$$

where ρ is the water density and g the gravitational acceleration. $S(\omega, \theta)$ is often referred to as the directional frequency spectrum and its unit is $m^2.Hz^{-1}.rad^{-1}$.

To illustrate the physical meaning of the directional frequency spectrum, it is useful to consider the wave field as a superposition of an infinite number of wave fronts of different frequencies travelling in different directions. Assuming linearity, the wave elevation $\eta(x, y, t)$ at a point of spatial coordinates (x, y) at time t is given by:

$$\eta(x,y,t) = \sum_{n=1}^{\infty} a_n \cos\left(k_n(x\cos\theta_n + y\sin\theta_n) - \omega_n t + \phi_n\right) \tag{18}$$

where the a_n's are the wave front amplitudes, the k_n's the wave numbers, the θ_n's the angles corresponding to the direction of propagation of the wave fronts, the ω_n's the angular frequencies, and the ϕ_n's the phases. If the ϕ_n's are distributed between 0 and 2π with a uniform probability density, $S(\omega, \theta)d\omega d\theta$ represents the contribution to the variance of the wave elevation due to wave components with frequencies between ω and $\omega + d\omega$ and directions between θ and $\theta + d\theta$:

$$S(\omega,\theta)d\omega d\theta = \sum_{\omega_n}^{\omega_n+d\omega}\sum_{\theta_n}^{\theta_n+d\theta}\frac{1}{2}a_n^2 \qquad (19)$$

It is common practice to decompose the directional variance spectrum as follows:

$$S(\omega,\theta) = S(\omega)D(\omega,\theta) \qquad (20)$$

where $S(\omega)$ is the "non-directional" variance spectrum which is related to $S(\omega, \theta)$ by:

$$S(\omega) = \int_0^{2\pi} S(\omega,\theta)d\theta \qquad (21)$$

and $D(\omega, \theta)$ is the Directional Spreading Function (DSF) which satisfies the two following properties:

$$D(\omega,\theta) \geq 0 \quad \text{for} \quad \theta \in [0, 2\pi] \qquad (22)$$

$$\int_0^{2\pi} D(\omega,\theta)d\theta = 1 \qquad (23)$$

Estimation of the directional frequency spectrum

The estimation of the directional frequency spectrum requires the measurement of a set of quantities associated with the wave field. The most common quantity recorded in a wave tank is the surface elevation. Elevation at one point is not sufficient to derive directional information and one has to record at least three different locations to do so. The directional frequency spectrum can also be computed from a single point measurement, but in this case other quantities have to be recorded in addition to surface elevation. This technique is typically used in the real sea using a heave-pitch-roll buoy. The present document focuses on multi-point surface elevation since it is the most widely used technique in wave tanks. More information on the other methods can be found in Benoit et al. [1997].

Most methods for estimating the directional frequency spectrum rely on the relationship between the cross-spectra of the surface elevation at different points and $S(\omega, \theta)$. We will assume that M wave gauges are used to measure simultaneously the surface elevation at M different locations. The cross-spectra or cross-covariance spectral density between two surface elevation signals η_p and η_q (from probes p and q with $p, q \leq M$ and $p \neq q$) is the Fourier transform of the cross-correlation between the two signals. Rigorous definitions of correlation and spectral density can be found in chapters 3 and 5 of Newland [2005], respectively. In the present context, the cross-correlation between η_p and η_q is defined by:

$$R_{pq}(\tau) = \lim_{T\to\infty}\frac{1}{T}\int_0^T \eta_p(t)\eta_q(t+\tau)dt \qquad (24)$$

and the corresponding cross-spectra by:

$$G_{pq}(\omega) = \int_{-\infty}^{+\infty} R_{pq}(\tau)e^{-i\omega\tau}d\tau \qquad (25)$$

Assuming linear wave theory and assuming that the phases of the different components of the wave field are randomly distributed, the relationship between the directional frequency spectrum and the cross-spectra is as follows:

$$G_{pq}(\omega) = \int_0^{2\pi} e^{-i\mathbf{k}\cdot(\mathbf{x}_q-\mathbf{x}_p)}S(\omega,\theta)d\theta \qquad (26)$$

$$\text{for} \quad p = 1,\ldots,M \quad \text{with} \quad p < q$$

The vector k is the wave number vector defined by:

$$\mathbf{k} = \begin{pmatrix} k\cos\theta \\ k\sin\theta \end{pmatrix} \qquad (27)$$

x_p and x_q are the vectors corresponding to the location of wave gauge p and q, respectively. It should be noted that (26) is more complex when the quantities measured at point p and q are different from surface elevation. More details on that topic can be found in Benoit et al. [1997].

Estimating the directional frequency spectrum involves computing the cross-spectra (25) from all the pairs of wave gauges and then inverting the relationship given by (26). The later operation is the most complex and tedious. With an infinite number of wave gauges, $S(\omega, \theta)$ can be in principle determined uniquely. In practice, there is only a finite number of probes (typically five to seven) and so the mathematical problem is not fully defined. Consequently some assumptions on $S(\omega, \theta)$ are required to yield a unique solution.

Several practical methods are available for estimating the directional frequency spectrum. None of them is perfect; they all have pros and cons. This document will briefly present and discuss the two most widely used. A more extensive review of the available methods can be found in Benoit et al. [1997].

The maximum likelihood method

The Maximum Likelihood Method (MLM) was originally introduced by Capon et al. [1967] in the field of seismic wave detection. The MLM relies on the assumption that the estimate of the directional frequency spectrum $\tilde{S}(\omega, \theta)$ can be expressed as a linear combination of the cross-spectra between the surface elevation measurements:

$$\tilde{S}(\omega,\theta) = \sum_{p=1}^{M}\sum_{q=1}^{M} \alpha_{pq}(\omega,\theta) G_{pq}(\omega) \qquad (28)$$

Expressing $G_{pq}(\omega)$ from (26) yields:

$$\tilde{S}(\omega,\theta) = \sum_{p=1}^{M}\sum_{q=1}^{M} \alpha_{pq}(\omega,\theta) \int_0^{2\pi} \qquad (29)$$

$$e^{-i\mathbf{k}'\cdot(\mathbf{x}_q-\mathbf{x}_p)} S(\omega,\theta')d\theta'$$

Where

$$\mathbf{k}' = \begin{pmatrix} k\cos\theta' \\ k\sin\theta' \end{pmatrix} \qquad (30)$$

(29) can be rewritten as:

$$\tilde{S}(\omega,\theta) = \int_0^{2\pi} w(\omega,\theta,\theta') S(\omega,\theta')d\theta' \qquad (31)$$

Where

$$w(\omega,\theta,\theta') = \sum_{p=1}^{M}\sum_{q=1}^{M} \alpha_{pq}(\omega,\theta) e^{-i\mathbf{k}'\cdot(\mathbf{x}_q-\mathbf{x}_p)} \qquad (32)$$

In (31), $\tilde{S}(\omega, \theta)$ can be seen as expressed as the convolution product of the true directional frequency spectrum by the window function $w(\omega, \theta, \theta')$. The more $w(\omega, \theta, \theta')$ tends toward a Dirac function, the better estimate $\tilde{S}(\omega, \theta)$ is of $S(\omega, \theta)$. Isobe and Kondo [1984] have shown that this is best achieved when:

$$\tilde{S}(\omega,\theta) = \frac{\kappa}{\sum_{p=1}^{M}\sum_{q=1}^{M} G_{pq}^{-1}(\omega)} \qquad (33)$$

where the $G_{pq}^{-1}(\omega)$ stands for the elements of the inverse of the cross-spectral matrix. The factor κ is derived by ensuring that the integral of $\tilde{S}(\omega, \theta)$ over the $[0, 2\pi]$ interval is equal to the measured non-directional variance spectrum (see equations (20) and (21)):

$$\int_0^{2\pi} \tilde{S}(\omega,\theta)d\theta = S_{measured}(\omega) \quad (34) \qquad \theta_k = \left(k - \frac{1}{2}\right)\Delta\theta \quad (35)$$

The MLM is often considered as one of the best methods for estimating the directional frequency spectrum and it is widely used. Benoit and Teisson [1994] have shown, however, that this method tends to overestimate the width of the directional peaks of the true spectrum.

It should be mentioned that the MLM does not perform as well in the presence of reflected waves. This is because reflection introduces phase locking (see *"Phase locking"* on page 63), which means that the phase of the different wave components forming the wave field are no longer randomly distributed. More details on the MLM performance with reflected waves can be found in Davidson et al. [1998].

The Bayesian directional method

The Bayesian Directional Method (BDM) relies on the Bayesian probability technique to estimate the directional frequency spectrum. The Bayesian approach was first introduced to wave directionality analysis by Hashimoto and Kobune [1988]. It has the advantage that it does not require any assumption on the shape of the Directional Spreading Function (DSF) except that it can be expressed as a piecewise constant function. It also accounts for potential errors in the cross-spectra computation.

The interval of definition [0, 2π] of the DSF is divided into K subintervals of equal width $\Delta\theta$ over which the estimate of the DSF $\tilde{D}(\omega, \theta)$ is assumed to be constant. A series $x_k(\omega)$ of K elements ($k = 1, ..., K$) is defined:

$$x_k(\omega) = \ln D(\omega,\theta_k) \quad \text{where}$$

from which the DSF can be approximated as follows:

$$\tilde{D}(\omega,\theta) = \sum_{k=1}^{K} I_k(\theta) e^{x_k(\omega)} \quad \text{where} \quad (36)$$

$$I_k(\theta) = \begin{cases} 1 & \text{when} \quad (k-1)\Delta\theta \leq \\ 0 & \text{otherwise} \end{cases}$$

Equation (36) is then inserted into (26) to yield a system of non-linear equations. The Bayesian method also includes a smoothness condition on the directional frequency spectrum function, which consists in minimizing the following quantity:

$$\sum_{k=3}^{K} (x_k - 2x_{k-1} + x_{k-2})^2 \quad (37)$$

The detailed derivation of the Bayesian directional method is complex and can be found in Hashimoto and Kobune [1988].

The BDM is very versatile and reliable and is, therefore, widely used. As for the MLM, it does not perform as well in the presence of reflected waves. More information on this topic can be found in Ilic et al. [2000] and Chadwick et al. [2000].

WAVE GENERATION

Two main classes of wave field are commonly generated in wave tanks: regular and irregular waves. The former type is simpler in that it is theoretically only associated with a limited number of parameters, namely one frequency and one amplitude. Tank testing of WECs in regular waves is very useful, especially in the

early design stage. It helps to gain a qualitative and quantitative understanding of the behaviour of the device in an environment controlled by only a few parameters. Regular waves are, however, virtually never encountered in the ocean and it is, therefore, important to also test WEC models in more "realistic" irregular waves.

To create irregular waves in a wave basin, an appropriate command signal needs to be sent to the wave-makers control system. The derivation of the command signal is basically done in two stages.

- A wave elevation time series corresponding to the desired target sea state (or spectrum) is computed.
- The wave tank "transfer function" is used to convert the above times series into the command signal.

The transfer function is the relation between the signal sent to the wave maker and the corresponding wave generated. Each wave basin has its own specific transfer function, which depends on its geometry and on the wave-makers geometry, dynamics, and drive system.

In most wave basins, the wave elevation time series is actually discrete and obtained by Inverse Discrete Fourier Transform (IDFT). The time series is computed by IDFT from the DFT complex coefficients (see equations (14) and (15)), which correspond to a target spectrum. The DFT coefficients can be derived according to different methods as will be explained in the following sections.

There are mainly two approaches to irregular wave generation. They are referred to as "deterministic" and "non-deterministic" or "probabilistic." The debate on which of these is better is perhaps more philosophical than technical and, to this day, there is still no widely acknowledged consensus on the topic. The authors will not venture in addressing the debate but will state the main advantages and disadvantages of each "school of thought." More arguments for this debate can be found in Funke and Mansard [1987] and Huntington [1987].

The Deterministic Approach

Random phase method

This method is based on the IDFT. The amplitude of the DFT coefficients are computed from the target spectrum so that they are proportional to the square root of the desired spectral density. The phase for each coefficient is chosen randomly. The random generation of the phase values is, however, initiated by a "seed" so that the series of phase values can be repeated identically at will by keeping the same seed number. The time series output from the IDFT is thus fully defined by the target spectrum and the seed number. This wave generation process is, therefore, considered deterministic. The length of the time series is often called the "repeat period" or "recycling length" of the command signal. More information on this method and its implementation can be found in Tuah and Hudspeth [1982].

Pros and cons of the deterministic approach

The main advantage of this method is that the discretized target spectrum can be guaranteed over the "repeat period." This allows reasonably short wave basin run times compared with the non-deterministic approach. The repeatability of wave trains generated is

also an advantage when carrying out comparative studies. The drawback of the deterministic approach is that it does not reproduce the true random behaviour of ocean waves. When using relatively short repeat periods, this can lead to "missing" some extreme events of low probability in the real world. The advocates of the deterministic approach argue that this issue can be overcome by generating extreme events separately in a deterministic manner. The supporters of the probabilistic method point out that such techniques imply assumptions by the experimenter of what an extreme event is. It is possible that phenomena other than large amplitude waves might generate extreme events for the wave power device studied. These could be, for example, a specific wave groupiness which, combined with the device dynamics leads to an extreme response. Such an extreme event would be difficult to predict.

The Non-Deterministic Approach

Random complex spectrum method

As for the random phase method, the random complex spectrum method relies on the IDFT. The complex DFT coefficients are computed from a target spectrum. They are obtained by multiplying the square root of the desired spectral density values by a random variable having a Gaussian distribution with zero mean and standard deviation of 1. This can be considered as "filtering" the random variable by the square root of the desired spectral density. More information on this method and its implementation can be found in Tuah and Hudspeth [1982].

White noise filtering method

The white noise filtering method consists in convoluting (or "filtering") a synthesized random number sequence (i.e. a white noise signal) with spectral values from the desired target spectrum. Applying the IDFT to the target spectrum yields the corresponding discrete time series. This time series can be considered as the coefficients of a digital filter, which is then applied to the white noise time series. The outcome is the command signal for the wave-maker control system. More on this method can be found in Bryden and Greated [1984].

The term "white noise" comes from the analogy with white light, whose spectrum is approximately constant over the range of visible frequency. The term noise comes from the field of electronics. White noise refers to a signal whose energy is evenly spread over the spectrum of interest.

Pros and cons of the non-deterministic approach

The realization of a sea state using this method will only match the target spectrum within the bounds of probability. In other words, the exact realization of the target spectrum is only guaranteed for runs of infinite duration. From a practical point of view, this means that experimental runs have to be rather long to properly represent the target spectrum. As an example, spectral shape for typical 20 minute realizations can deviate very significantly from the target spectrum [Miles and Funke, 1989].

All the realizations of a same target spectrum will be different, although statistically similar. This might not be appropriate for comparing the performance of different devices under similar sea states. On the other hand, the spectral shape obtained will have similar statistical variability to that of real ocean waves over the same duration.

Wave Tank Calibration

A wave tank transfer function "translates" the wave elevation command signal to the wave-makers into physical wave heights in the basin. The theoretical derivation of such transfer functions was pioneered by Biesel and Suquet [1951] for piston and flap type wave-makers controlled in displacement.

When working with regular waves, the quantities investigated are often "normalized" by the measured wave height. This approach tends to limit the impact of inaccuracies in the transfer function in the sense that even if the height of the generated waves is slightly different from the target height, at least the actual wave height is known and taken into account through the "normalization" process. The accuracy of the transfer function is, however, particularly important when working with irregular waves. If, for some frequencies, the height of the waves generated does not correspond to the target height, the actual energy spectrum will be distorted compared to the target one.

If a theoretically derived transfer function is a good starting point, it is worth refining it through experimental wave tank calibration.

As an example, with Edinburgh Designs Limited wave making systems, the tank transfer function file requires specifying gain values for discrete wave frequencies and discrete wave heading angles [Rogers and Bolton King, 1997]. The gain relates the target wave height with the voltage of the command signal for the wave frequency and heading angle considered. The more gain values are specified, the better the transfer function. Covering the whole frequency spectrum and angle range with a fine resolution can, however, prove long and tedious. It is, therefore, possible to only specify a limited number of gain values and let the wave-maker control system interpolate between these.

When carrying out the calibration, it is recommended to process the wave elevation time series recorded using a wave reflection analysis technique. Since only a single direction of wave propagation is considered at a time, a two dimensional method is generally considered sufficient (see *"Two-dimensional wave reflection"* on page 54).

The gain is generally linearly related to the height of the waves generated. Calibration for a single frequency and angle can, therefore, be achieved with a single set of measurements by adjusting the gain linearly with the error between the target wave height and the measured value. To achieve a more accurate calibration, an iterative method can be adopted.

Figure 7 shows the measured energy spectra for a long crested modified Pierson Moskowitz sea generated in the Edinburgh Curved tank before (a) and after (b) calibration. Measurements have been carried out by Jorge Lucas. He has used the two dimensional Mansard and Funke reflection analysis method (see *"Two-dimensional wave reflection"* on page 54) to separate the incident from the reflected waves. The improvement brought about by the calibration is very significant.

Phase Locking

Phase locking is a phenomenon happening when regular waves of equal frequency and with constant phase shift between each other are superposed. The direction of propagation

of these waves can be different. The resulting wave field is affected by patterns of nodes and antinodes, which makes it spatially inhomogeneous and non-ergodic. This means, among other things, that the statistical properties of quantities linearly associated with this wave field will be different from one point of the wave field to another. More details on the impact of non-ergodicity and inhomogeneity can be found in Jefferys [1987].

The simplest example of phase locking can be observed when a regular wave hits perpendicularly a fully reflective vertical wall. A reflected wave of equal frequency and amplitude travelling in the opposite direction forms. The phases of the incident and reflected waves are locked by the fact that they are both equal on the wall. The resulting wave pattern is that of a standing wave with nodes and antinodes. When measuring the wave height of a standing wave, the value obtained will be strongly affected by the spatial location at which the measurement is taken. At a node, the wave height will almost be zero whereas at an antinode, it will be maximum (about twice the height of the incident regular wave).

Phase locking is an important phenomenon to be aware of when carrying out model testing in a wave tank. Wave basins are by nature bounded fluid domains and no beach or wave-maker has perfect absorption characteristics. The wave field generated in the tank will be inevitably affected by reflections and thus phase locking. The scale of the non-ergodicity and spatial inhomogeneity due to wave reflection depends on many parameters including tank geometry, presence of reflecting side walls, reflection characteristics of the

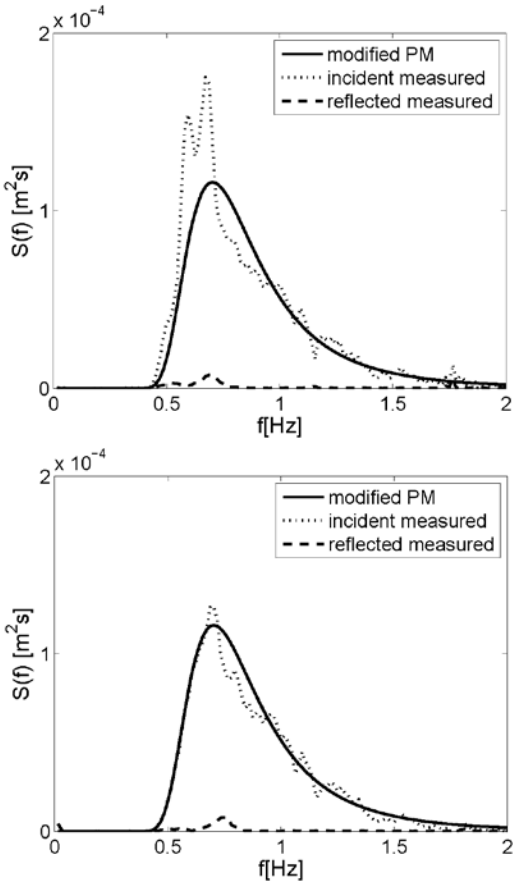

Figure 7: Realizations of a modified Pierson Moskowitz spectrum before (a) and after (b) wave tank calibration. The solid line corresponds to the target spectrum, the dotted line to the incident measured spectrum, and the dashed line to the reflected measured spectrum.

beach at the wave frequency considered, and the heading angle of the wave generated. It is, therefore, advisable to "map" the tank to find out which parts of it are the least affected by reflection for given wave conditions and, therefore, the most suitable to locate the model to be investigated. Before model testing, it is also recommended to measure the waves in the absence of the model at the location where the model is to be placed to ensure that they correspond to the target wave conditions [ITTC, 2005].

Lack of spatial homogeneity can have a significant impact when investigating the behaviour of a free-floating wave energy

device in a wave basin, especially if the mooring is compliant. Drift force and low frequency mooring oscillations can move the model away from its original position and, if the wave field is not homogenous "enough," the model might end up being subjected to waves whose characteristics are different from those of the waves recorded at the original location of the model.

When generating multi-directional irregular seas, phase locking can be an issue. This depends on which generation technique is used

Double summation method

The double summation method was originally the most commonly used approach for generating multi-directional spectra. With this technique, the target wave height η is defined as follows:

$$\eta(x,y,t) = \sum_{i=1}^{N}\sum_{j=1}^{M} A_{ij}\cos\left(\omega_i - k_i(x\cos\theta_j + y\sin\theta_j) + \phi_{ij}\right) \quad (38)$$

where x and y are horizontal spacial coordinates, t is time, the A_{ij}'s are the amplitudes of the wave components, the ω_i's are the discrete radian frequencies of the wave components, the k_i's are the corresponding wave numbers, the θ_j's are the heading angles of the wave components, and the $\emptyset_{ij}$'s are the phases.

From equation (38), the target spectrum is made of $N \times M$ wave fronts spread over N discrete frequencies and M discrete angles. The main limitation of this method lies in the fact that for each frequency ω_i there are M wave fronts of different direction with exactly that same frequency. This leads to phase locking. The resulting spatial inhomogeneity can be significant. Jefferys [1987] carried out numerical simulation of a $cos^2\,\theta$ directional sea with 36 phase locked wave components. He found that over an area of one square kilometre, the mean energy at 0.1 Hz computed from wave elevation varies between zero and four times the spatial mean value.

There are ways to improve the ergodicity and the spatial homogeneity of the double summation method. Miles and Funke [1989] present a method which consists in increasing the number of discrete frequencies in the spectrum definition given by (38). Instead of expressing each frequency bin of the target spectrum by a single frequency component, the bins are represented by P frequency components each. These frequencies ω_{iq} are defined as follows:

$$\omega_{iq} = \left(\omega_i - \frac{\Delta\omega}{2}\right) + q\frac{\Delta\omega}{P} \quad \text{for} \quad q = 1,\ldots,P \quad (39)$$

where ω_i is the same as in (38) and $\Delta\omega$ is the width of the bin.

Miles and Funke [1989] have then numerically investigated the variability of the variance of wave elevation η and of the cross-spectra. They have found that ergodicity and homogeneity can be improved by increasing the value of P, but this also increases the computational burden involved. They also point out that the length of the record used to compute the cross-spectra has a significant impact on the variability. Variability can also be reduced by ensemble averaging over several realizations [Jefferys, 1987].

Single summation method

A multi-directional irregular sea-state generated by the single summation method has only one wave component at any particular frequency. The target wave height η is defined as follows [Miles and Funke, 1989]:

$$\eta(x,y,t) = \sum_{i=1}^{N\times M} A_i \cos\left(\omega_i - k_i(x\cos\theta_i + y\sin\theta_i) + \phi_i\right) \quad (40)$$

where $\omega_i = i\,\frac{\Delta\omega}{M}$ with M being the number of heading angles. The θ_i's are defined so that all the M heading angles are included in each frequency bin of width $\Delta\omega$. In other words, each bin of width $\Delta\omega$ is split into M equally wide segments with a single wave component per segment. The M wave components of a bin correspond to the M heading angles and they all have slightly different frequencies.

With all the wave components having different frequencies, there is no phase locking and the sea state generated is spatial homogenous and ergodic. The quality of the waves generated with this method will improve with increasing M and decreasing $\Delta\omega$, but values of these parameters can be limited by the angular and frequency resolutions of the wave-making system. Miles and Funke [1989] carried out numerical simulation and found out that the derivation of the cross spectra will be "reasonably accurate" with $M = 32$ and $\Delta f = 0.04$ Hz with $\Delta f = \frac{\Delta\omega}{2\pi}$. Miles and Funke [1989] point out that the maximum wave heights in sea states generated with this method may tend to be smaller than those of a corresponding realization in a real sea.

Numerical Wave Basins

In 1989, Grilli et al. [1989] put forward the idea of a Numerical Wave Tank (NWT). The principal idea was to develop a flow solver capable of simulating the processes normally studied experimentally in a physical wave tank. Early attempts to develop NWTs were normally restricted to 2D simulations for reasons of computational efficiency. Increasing computer power, however, has led to the development of three dimensional numerical wave basins. The requirement is to develop a numerical scheme capable of accurately solving a problem involving the resolution of a moving material interface, whose location not only depends on the local flow solution, but also has a major influence on it [Li et al., 2004]. Under the action of breaking waves, the free surface undergoes gross topological changes with both merging and breakup. The simulation of such processes requires a powerful numerical tool with the ability to handle arbitrarily shaped non-contiguous interfaces.

A number of approaches are available, including the density function method [Park et al., 1999]; a front-tracking approach [Unverdi and Tryggvason, 1992]; smoothed particle hydrodynamics [Monaghan, 1994]; the level set method [Osher and Sethian, 1998]; the volume of fluid method [Hirt and Nichols, 1981]; and the free-surface capturing approach [Kelecy and Pletcher, 1997]. In addition, turbulence effects play an important role, particularly in the surf zone, and this can be modeled either using Large Eddy Simulation [Watanabe et al., 2008] or a Reynolds-Averaged approach [Lin and Liu, 1998]. Most of these approaches simplify the flow problem and the computational requirements by

considering only the liquid-component (modeling the gas component by a numerical vacuum). A number of commercial computational fluid dynamics codes (e.g. Star-CCM+) provide facilities for implementing "Numerical Towing Tanks" and have been applied to some quite complex wave/structure interaction problems (e.g. [Parsons and Kotinis, 2008]).

Such methods which solve the three-dimensional Navier-Stokes equations are highly computationally demanding so simulations are normally limited to the interaction of between one and ten waves with a model of wave energy converter. Such simulations provide a vast amount of information about the fluid motion, allowing effects such as vortex generation to be examined in detail. The authors note that the combination of detailed numerical modeling and physical experiments is extremely powerful in aiding understanding of how a machine performs. We add the caveat that simulations must be conducted rigorously following a series of quality control protocols and require skilled interpretation, and note that such protocols are beyond the scope of this paper.

More computationally efficient models normally use simplified flow models and are based on the potential flow equations [Grilli et al., 1989], shallow water equations [Shiach et al., 2004], or a two dimensional vertical formulation [Qian et al., 2005].

CONCLUSIONS

It is undoubtedly true that high quality experimental programs are an invaluable tool in the assessment, design, and optimization of wave energy converters. There is a considerable history of such programs in established research groups around the world. This paper has attempted to draw together elements of best practice in the performance of such experiments in the hope that new comers to the field will not repeat previous mistakes and thus minimize the time and effort required to develop a new concept.

The authors strongly recommend that the evaluation of any wave energy concept is conducted in a well calibrated facility, ideally with absorbing wave makers. Initial tests should be conducted at the smallest practical scale, moving on to large scales and more realistic moorings and PTOs once the fundamental concept of the device has been proven. Testing should commence with regular, long crested waves before progressing to more realistic irregular, mixed seas. The sampling rates for measurements must be selected to prevent aliasing and spilling. Finally we note that a wide range of measurement instruments and sensors are available (more than are summarized in this paper) and the user must be familiar with the performance of any instrument that they are using.

ACKNOWLEDGEMENTS

This review work has been supported by the UK Engineering and Physical Sciences Research Council through the SuperGen2 Marine Research Consortium. The authors would like to thank Matthew Folley from Queen's University Belfast for his helpful contribution.

David Ingram wishes to acknowledge support for his position from the Scottish Funding Council and for their support of the Joint Research Institute in Energy with the Heriot-

Watt University as a component part of the Edinburgh Research Partnership.

REFERENCES

AEA Energy and Environment [2006]. *Review and analysis of ocean energy systems developing and supporting policies*. Report on behalf of Sustainable Energy Ireland for the IEA-OES.

Benoit, M. and Teisson, C. [1994]. *Laboratory comparison of directional wave measurement systems and analysis techniques*. Proceedings of the 24th International Conference on Coastal Engineering. Kobe, Japan, pp. 42-56.

Benoit, M., Frigaard, P., and Schaffer, H.A. [1997, August]. *Analysing multidirectional wave spectra: A tentative classification of available methods*. IAHR Seminar on Multidirectional Waves and their Interaction with Structures. San Francisco, US, pp. 131-158.

Biesel, F. and Suquet, F. [1951]. Les appareils generateurs de houle en laboratoire. *La Houille Blanche*, Vol. 6, No. 2, pp. 147-165.

Bryden, I.G. and Greated, C.A. [1984]. Generation of three-dimensional random waves. *Journal of Physics D: Applied Physics*, Vol. 17, No. 12, pp. 2351-2366.

Capon, J., Greenfield, R., and Kolker, R. [1967]. *Multidimensional maximum-likelihood processing of large aperture seismic array*. IEEE Proceedings Vol. 55, No. 2, pp. 192-211.

Chadwick, A., Ilic, S., and Helm-Petersen, J. [2000]. Evaluation of directional analysis techniques for multidirectional, partially reflected waves, part 2: application to field data. *Journal of Hydraulic Research*, Vol. 38, No. 4, pp. 253-258.

Clayson, C. [1989]. *Survey of instrumental methods for the determination of high-frequency wave spectrum*. Technical Report 267, Institute of Oceanographic Sciences Deacon Laboratory. Retrieved from http://eprints.soton.ac.uk/15285/01/267.PDF.

Cooley, J. and Tukey, J. [1965]. An algorithm for the machine calculation of complex Fourier series'. *Mathematics of Computation*, Vol. 19, pp. 297-301.

Davidson, M.A., Huntley, D.A., and Bird, P.A. [1998]. Practical method for the estimation of directional wave spectra in reflective wave fields. *Coastal Engineering*, Vol. 33, No. 2-3, pp. 91-116.

Funke, E. and Mansard, E. [1987, September]. *A rationale for the use of the deterministic approach to laboratory wave generation*. IAHR Seminar on WaveAVE Analysis and Generation in Laboratory Basins, Lausanne, Switzerland, pp. 153-195.

Goda, Y. and Suzuki, Y. [1976]. *Estimation of incident and reflected waves in random wave experiments*. 15th Coastal Engineering Conference, pp. 828-845.

Grilli, S.T., Skourup, J., and Svendsen, I. [1989]. An efficient boundary element method for nonlinear water-waves. *Engineering Analysis with Boundary Elements*, Vol. 6, No. 2, pp. 97-102.

Hashimoto, N. and Kobune, K. [1988]. *Directional spectrum estimation from a Bayesian approach*. 21st Coastal Engineering Conference, Malaga, Spain, pp. 62-76.

Hirt, C. and Nichols, B. [1981]. Volume of fluid methods for dynamics of free boundaries. *Journal of Computational Physics*, Vol. 39, pp. 201-225.

Horowitz, P. and Hill, W. [1989]. *The art of electronics*. Cambridge University Press.

Huntington, S. [1987, September]. *A rationale for the use of the probabilistic approach to laboratory wave generation*. IAHR Seminar on Wave Analysis and Generation in Laboratory Basins, Lausanne, Switzerland, pp. 197-208.

Ilic, S., Chadwick, A. and Helm-Petersen, J. [2000]. Evaluation of directional analysis techniques for multidirectional, partially reflected waves, part 1: numerical investigations. *Journal of Hydraulic Research*, Vol. 38, No. 4, pp. 243-251.

Isaacson, M. [1991]. Measurement of regular wave reflection. *Journal of Waterway, Port, Coastal and Ocean Engineering*, Vol. 117, No. 6, pp. 553-569.

Isobe, M. and Kondo, K. [1984]. *Method for estimating directional wave spectrum in incident and reflected wave field*. Proceedings of the 19th International Conference on Coastal Engineering, pp. 467-483.

ITTC [2005]. *Testing and Extrapolation Methods, Loads and Responses, Ocean Engineering, Floating Offshore Platform Experiments*. International Towing Tank Conference – Recommended Procedures and Guidelines, No. 7.5-02-0703.1. Retrieved from http://ittc.sname.org.

Jefferys, E.R. [1987]. Directional seas should be ergodic. *Applied Ocean Research*, Vol. 9, No. 4, pp. 186-191.

Jeffrey, D.C., Richmond, D.J.E., Salter, S.H., and Taylor, J.R.M. [1976]. *Study of mechanisms for extracting pover from sea waves*. Technical report, University of Edinburgh. Retrieved from www.see.ed.ac.uk/~ies/Wave_power_group_reports/EWPP%202nd%20year%2report%20OCR%20reduced%20plus%20photos.pdf.

Kelecy, F. and Pletcher, R. [1997]. The development of a free surface capturing approach for multidimensional free surface flows in closed containers. *Journal of Computational Physics*, Vol. 138, pp. 939-980.

Li, T., Troch, P. and De Rouck, J. [2004]. Wave overtopping over a sea dike. *Journal of Computational Physics*, Vol. 198, No. 2, pp. 686-726.

Lin, P. and Liu, P. [1998]. A numerical study of breaking waves in the surf zone. *Journal of Fluid Mechanics*, Vol. 359, pp. 239-264.

Lucas, J., Cruz, J., Salter, S., Taylor, J.R.M., and Bryden, I.G. [2007, September]. *Update on the modeling of a 1:33 scale model of a modified Edinburgh duck WEC*. 7th European Wave and Tidal Energy Conference, Porto, Portugal.

Mansard, E.P.D. and Funke, E.R. [1980]. *Measurement of incident and reflected spectra using a least squares method*. 17th International Conference on Coastal Engineering, Sydney, Australia, pp. 95-96.

Mansard, E.P.D. and Funke, E.R. [1987, September]. *Experimental and analytical techniques in wave dynamics, a comparative study*. IAHR Seminar on Wave Analysis and Generation in Laboratory Basins, Lausanne, Switzerland, pp. 91-116.

Maunsell, C. and Murphy, T. [2005]. *Effects of air compressibility in oscillating water column physical modeling*. Technical report, University College Cork, Final year project report at HMRC.

Miles, M. and Funke, E. [1989]. Comparison of methods for synthesis of directional seas. *Journal of Offshore Mechanics and Arctic Engineering*, Vol. 111, No. 1, pp. 43-48.

Monaghan, J. [1994]. Simulating free surface flows with SPH. *Journal of Computational*

Physics, Vol. 110, pp. 499-406.

Mueller, M. and Jeffrey, H. [2008]. *UKERC marine (wave and tidal current) renewable energy technology roadmap*. Retrieved from http://ukerc.rl.ac.uk/Roadmaps/Marine/Tech_roadmap_ summary%20HJMWMM.pdf.

Nebel, P. [1994]. *Synthesis of optimal control of a wave energy converter*. Ph.D. thesis, University of Edinburgh.

Newland, D. [2005]. *An introduction to random vibrations, spectral and wavelet analysis*, 3rd Edition. Dover Publications.

Newman, J. [1977]. *Marine hydrodynamics*. The MIT Press.

Osher, S. and Sethian, J. [1998]. Fronts propagating with curvature-development speed: algorithm based on Hamilton-Jacobi formulations. *Journal of Computational Physics*, Vol. 79, pp. 12-49.

Park, J., Kim, M., and Miyata, H. [1999]. Full non-linear free-surface simulations by a 3D viscous numerical wave tank. *International Journal for Numerical Methods in Fluids*, Vol. 29, No. 6, pp. 658-703.

Parsons, M. and Kotinis, M. [2008]. *Further development and optimization of the ballast-free ship Design concept*. Great Lakes Maritime Research Institute, University of Michigan.

Qian, L., Mingham, C., Causon, D., Ingram, D., Folley, M., and Whittaker, T. [2005]. Numerical solution of wave power devices using a two-fluid free surface solver. *Modern Physics Letters*, Vol. B19, pp. 51-54.

Rogers, D. [1987, August]. *Development of sonar ranging techniques for three dimensional measurements in mixed sea basins*. Technical report, University of Edinburgh. Retrieved from www.see.ed.ac.uk/~ies/Wave_power_group_reports/SONAR%20RANGING%201987.pdf.

Rogers, D. and Bolton King, G. [1997]. *Wave generation using ocean and wave*. Edinburgh Designs Ltd., Edinburgh, Scotland. Retrieved from www.edesign.co.uk.

Salter, S., MacGregor, K., and Jones, C. [2006]. *Scottish energy review, Scotland's opportunity – Scotland's challenge*. Retrieved from www.see.ed.ac.uk/~shs/Energy%20review/Energy% 20review.pdf.

Sarpkaya, T. and Isaacson, M. [1981]. *Mechanics of wave forces on offshore structures*. Van Nostrand Reinhold.

Shiach, J., Mingham, C., Ingram, D., and Bruce, T. [2004]. The applicability of the shallow water equations for modeling violent wave overtopping. *Coastal Engineering*, Vol. 51, No. 1, pp. 1-15.

Spinneken, J. [2004]. *Water surface following wave gauge*. Technical report, University of Edinburgh. Retrieved from www. wavegauge.joecraft.com.

Stansfield, F. [1970]. *Hydrostatic bearings*. The Machinery Publishing Company Ltd.

Taylor, J. and Mackay, I. [2001, March]. *The design of an eddy current dynamometer for a free-floating sloped IPS buoy*. Marine Renewable Energy Conference, The Institute of Marine Engineers, Newcastle upon Tyne, UK, pp. 67-74.

Thompson, E.F. and Long, C.E. [1987, September]. *Wave measurement and analysis in laboratory flumes*. IAHR Seminar on Wave Analysis and Generation in Laboratory Basins, Lausanne, Switzerland, pp. 75-90.

Thornton, E.B. and Calhoun, R.J. [1972]. Spectral resolution of breakwater reflected waves. *American Society of Civil Engineers, Journal of the Waterways, Harbors and Coastal Engineering Division 98 (WW4)*, pp. 443-460.

Tuah, H. and Hudspeth, R.T. [1982].

Comparisons of numerical random sea simulations. *Journal of Waterway, Port, Coastal and Ocean Engineering 108 (WW4)*, pp. 569-584.

Unverdi, S. and Tryggvason, G. [1992]. A front-tracking method for viscous, incompressible multifluid flow. *Journal of Computational Physics*, Vol. 100, pp. 25-37.

Watanabe, Y., Saruwatari, A., and Ingram, D. [2008]. Free-surface flows under impacting droplets. *Journal of Computational Physics*, Vol. 227, No. 4, pp. 2344-2365.

Weber, J. [2007, September]. *Representation of non-linear aero-thermodynamic effects during small scale physical modeling of OWC WECs*. 7th European Wave and Tidal Energy Conference. Porto, Portugal.